Design, fabrication and characterization of whispering-gallery mode miniature sensors

Haiyong Quan[a], Zhixiong Guo[*a], Lei Xu[a], Stanley Pau[b],
[a]Dept. of Mech. & Aerosp. Eng., Rutgers University, 98 Brett Road, Piscataway, NJ, USA 08854
[b]Nanofabrication Research Laboratory, Lucent Technologies/Bell Labs., Murray Hill, NJ, 07974

ABSTRACT

In this paper, we present the design, fabrication and characterization of the whispering-gallery mode (WGM) miniature sensors for potential use in biosensing at the nanometer scale. In order to understand and investigate the characteristics of WGM resonances, we designed and fabricated a number of sensors with different dimensions. Each sensor is a micro/nano-structure consisted of a microdisk as the resonating cavity and a micro waveguide for light delivery and collection. In addition to the waveguides having uniform cross-section dimensions, tapered waveguide was also considered in our studies. A simulation model was employed to characterize the EM field and radiation energy density of the designed sensors. The gap effects on WGM resonance in terms of quality factor and full width at half maximum (FWHM) were evaluated. Following the design and characterization, the sensors were fabricated in 1.3μm-thick Si_3N_4 film using 248nm optical lithography and conventional silicon IC processing. Top and down SEM measurements of the fabricated sensors were conducted and the data for the sensors in one device are given.

Keywords: Whispering-gallery mode, sensors, micro/nano-structures, design, nanofabrication, waveguide, optical lithography, optical resonance, measurement, simulation.

1. INTRODUCTION

Whispering-gallery mode (WGM) is a particular mode of microcavity resonances. It occurs when light at certain frequencies travels in a dielectric medium of circular geometry[1]. After repeated total internal reflections at the curved boundary the electromagnetic field can close on itself, giving rise to resonances. The resonances were first observed in dielectric spheres by Ashkin and Dziedzic[2] in their experiments related to particle levitation and radiation pressure. Theoretically, WGM resonances in spheres can be obtained via a detailed solution of electromagnetic (EM) wave equations[3,4]. The resonant wavelengths and frequencies can be estimated using the following approximation:

$$2\pi r \approx \frac{m\lambda_m}{n} = \frac{mc_0}{f_m n} \tag{1}$$

where r and n are the radius and refractive index of the microcavity, respectively; m is an integer and represents the resonance mode; λ_m and f_m are the resonant wavelength and frequency at mode m, respectively. If a dielectric medium has a dimension of the order of the wavelength, $r \sim \lambda_m$, and has negligible optical loss, a microcavity made of this medium can have a very small mode volume and high finesse.

WGMs have received increasing attention due to their high potential for realization of microlasers[5,6], optical biosensors[7], narrow filters[8], optical switching[9], and high resolution spectroscopy[10], etc. In recent years, for example, WGM miniature biosensors have been attracting many research efforts because of the need for sensitive sensors in life sciences, drug discovery, and homeland security. Usually, optical resonance techniques can be used to enhance the sensitivity of biosensor devices. WGM sensors can possess high sensitivity and selectivity, small sample volume, and robustly integrated properties to be fabricated in a lab-on-a-chip device. The sensors can also be used for identifying and monitoring proteins, DNA, peptides, and toxin molecules at the nanometer scale[11-14].

There are several configurations of WGM devices. The microcavity can be of any circular geometries like spheres, disks, and rings. The diameter of the considered microcavities varies from several micrometers to hundreds of micrometers. Phase-matched optical waveguides or optical fiber cores are usually utilized to deliver light into the cavity

* guo@jove.rutgers.edu; phone 1 732 445-2024; fax 1 732 445-3124

Nanofabrication: Technologies, Devices, and Applications, edited by Warren Y-C. Lai, Stanley Pau, O. Daniel López, Proc. of SPIE Vol. 5592 (SPIE, Bellingham, WA, 2005)
0277-786X/05/$15 · doi: 10.1117/12.571303

and to collect signals for measuring WGM resonant frequencies. Any shift and broadening in the resonances signify change of the cavity environment. The waveguide(s) or fiber core(s) should not be in direct contact with the resonating microcavity to avoid disturbing the orbiting of photons. Photons may orbit the periphery of the microcavity thousands of times before exit[1]. On the other hand, the gap separating the microcavity and the waveguide(s)/fiber core(s) must be less than one optical wavelength in order to maintain an evanescent field connecting the microcavity and the waveguide(s)/fiber core(s). Thus, WGM resonators are typical devices of micro/nano-opto-mechanical systems (MOMS or NOMS) where an optimal gap distance may exist.

Many researchers built WGM sensors using microsphere and eroded optical fiber coupling structure. For example, Arnold's group discovered WGM resonances and morphology-dependence[15] in this structure and applied it for their biosensing studies[12-14]. The microspheres considered were usually in the size range of several hundreds of micrometers. They used single mode optical fibers. The fiber cladding was eroded and etched to the limit such that an evanescent field exists, but there is no transmission loss. The microsphere was coupled to the fiber with the assistance of a stereo microscope. Some other researchers[16-18] considered the use of tapered optical fibers. Knight et al.[16] showed that high-Q WGMs can be efficiently excited by an optical fiber taper. They made fiber tapers by means of heating and stretching. Such configurations of microsphere-fiber coupling design are easy to realize in individual labs. The fibers are flexible and convenient for inputting excitation light and receiving signals. However, it is very difficult to control the radial size of the fiber tapers and the coupling gap distance between the eroded fiber (or fiber taper) and the microsphere. Difficulties in mass production and uniformity make this configuration less attractive for use as practical sensors.

The rapid advances in modern micro/nano-fabrication techniques have made it feasible to consider WGM microcavity resonances in fine and uniform devices having physical dimensions at micro- and nanometer scales. Micro/nano-fabricated waveguides were adopted for replacing optical fibers. Integration of microcavities and waveguides can be easily achieved through fabrication methods like optical lithography, chemical vapor deposition (CVD), and chemical or plasma etching. Dimensions of 100-200 nm are routinely achieved in the manufacturing of integrated circuits. For example, Zhang et al.[19] realized an InGaAsP photonic-wire microcavity ring laser consisting of a ring cavity of 4.5-μm in diameter and a curing waveguide of 0.4-μm width. Laine et al.[20] considered microsphere and waveguide coupler in their acceleration sensor design. Klunder et al.[21] designed laterally and vertically waveguide-coupled cylindrical micro-resonators in Si_3N_4 on SiO_2 technology using conventional optical lithography. Krioukov et al.[22] examined integrated optical microcavity sensors. Belarouci et al.[23] conducted design and simulation of high-Q ring resonators coupled to submicron-width waveguides based on the nanofabrication of TiO_2-SiO_2 sol-gel thin films. The waveguide and microcavity coupling design and semiconductor nanofabrication techniques allow us to produce WGM sensors in volume and ensure uniformity in manufacture. Compactly integrated and robust lab-on-a-chip WGM devices are then manufacturable.

Our research group is currently studying nano-biophotonics with emphasis on the development of sensing techniques and devices for bio-molecular detection and identification at the nanometer scale. To explore the use of WGM phenomena as novel sensing tools at the nanometer scale, it is necessary to perform parametric studies to systematically investigate the influences of microcavity size and material, gap distance separating waveguide and microcavity, waveguide size and shape, and cladding material for waveguide, etc. These studies are conducted both experimentally and numerically. We will report our simulation studies in another paper[24] in the conference. In this paper, we present the design and fabrication of the WGM miniature sensors that will be used for experimental studies. Characterization of the designed sensors is performed using our simulation model to examine the design. The operating resonance frequency is chosen within the near infrared range, in which the spectrum is the so-called "optical window" for biologic tissues and the absorption of bio-solutions is usually very weak. Following the design and characterization, the fabrication procedure will be introduced, and the SEM measurement data of the fabricated WGM sensor will be presented.

2. DESIGN

Taking variation in Eq. (1), it follows that

$$\frac{\Delta f}{f} + \frac{\Delta r}{r} + \frac{\Delta n}{n} \approx 0 . \qquad (2)$$

When bio-molecules are adsorbed or attached to the peripheral surface of the cavity, it will change the cavity radius and, consequently, shift the resonant frequency. The frequency shift of a given resonant mode assuming constant refractive index is estimated as: $\Delta f / f \approx -\Delta r / r$. If we consider the linewidth of the resonance to be the smallest measurable shift (taken as $\Delta f = 10$ MHz for the state-of-the-art instrument, $f = 3.75\times10^{8}$ MHz at $\lambda = 800$ nm), then the smallest "measurable" size change is $|\Delta r|_{\min} = 2.6\times10^{-8} r$. With the radius $r \sim 10^{4}$ nm in typical miniature resonators, $|\Delta r|_{\min} = 2.6\times10^{-4}$ nm — a value smaller than the size of an atom is theoretically detectable! In the present studies, we considered a linewidth of 0.01 nm.

We need to find whispering-gallery modes and frequency shifts against cavity geometry changes in the operating wavelength range of 790 - 820 nm. The material to be used must be low loss and susceptible to chemical surface modifications used in our biosensing studies. Other design criteria include cost of fabrication using the available facilities at Lucent Technologies/Bell Labs., and simple configuration for easy light alignment, coupling, and measurement.

The sketch of one designed sensor is shown in Fig. 1. The sensor is an integrated waveguide and microdisk device to be fabricated on silicon wafers. Silicon Nitride (Si_3N_4) was selected as the sensor material for waveguide and microdisk because this substance has excellent physical and thermal stability, low cost[25], and extremely low optical absorption around the operating wavelengths[26]. The designed thickness of the sensor was 2μm. A 3μm-thick layer of SiO_2 is employed as the low cladding of the device. These thin films can be deposited on the surface of silicon wafer by using the low-pressure chemical vapor deposition (LPCVD) or the plasma-enhanced chemical vapor deposition (PECVD). The large refractive index of Si_3N_4 (about 2.01 around 800nm) ensures high contrast of refractive indices between the WGM resonator and its surrounding medium (air or bio-solutions) and may result in high-quality resonance modes. Of course, this large refractive index waveguide faces challenges in light coupling.

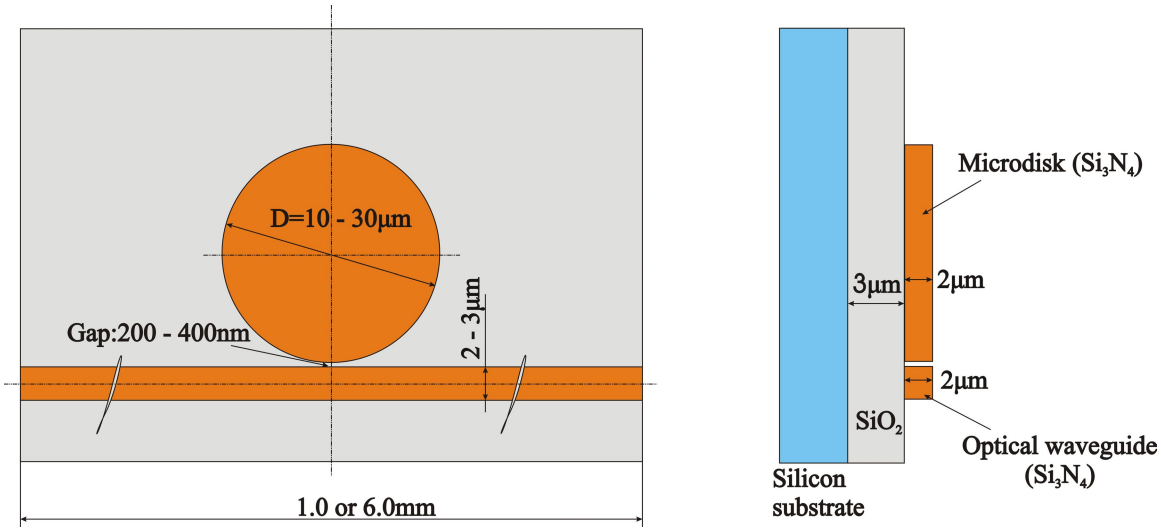

Figure 1. Sketch of the sensor design.

Polymer materials may have a high potential to be used as WGM biosensors because of their appealing features like close affinity with bio-molecules and low cost in mass production for integrated photonic systems[27]. However, the use of polymer materials often result in more thermally sensitive components as compared with glass or semiconductor based counterparts. For thermally sensitive materials, both the microcavity radius and refractive index are strong functions of temperature. If polymer materials were to be used as WGM sensing materials, precise control of the operating temperature would be a big issue.

To investigate the dimension effects of WGM sensors, we designed a number of sensors with different dimensions. Figure 2 displays the layout of the sensors in a square stepper with maximum square die size of 22mm. After fabrication, the die is cut into two chips of equivalent die size. In order to avoid possible excessive attenuation of light intensity in the waveguide, the waveguides in one chip are 1mm long, while they are 6mm long in another chip. Other parameters are identical for the two chips. There are 12 parallel miniature resonators in each of the chips. The vertical interval between adjacent sensors is 1mm to avoid interference in experimental measurements. The centers of the microdisks in the device are aligned with the mid-points of the waveguides.

The gap which is defined as the minimal separating distance between the microdisk and waveguide varies from 200, 300, to 400nm. The diameter of the microdisks varies between 10 and 30μm. In each chip, there are eight straight waveguides and four tapered waveguides. However, the width of the waveguides in a 100μm-long central segment remains constant and is either 2 or 3μm. The width at both ends of the tapered waveguides is 10μm.

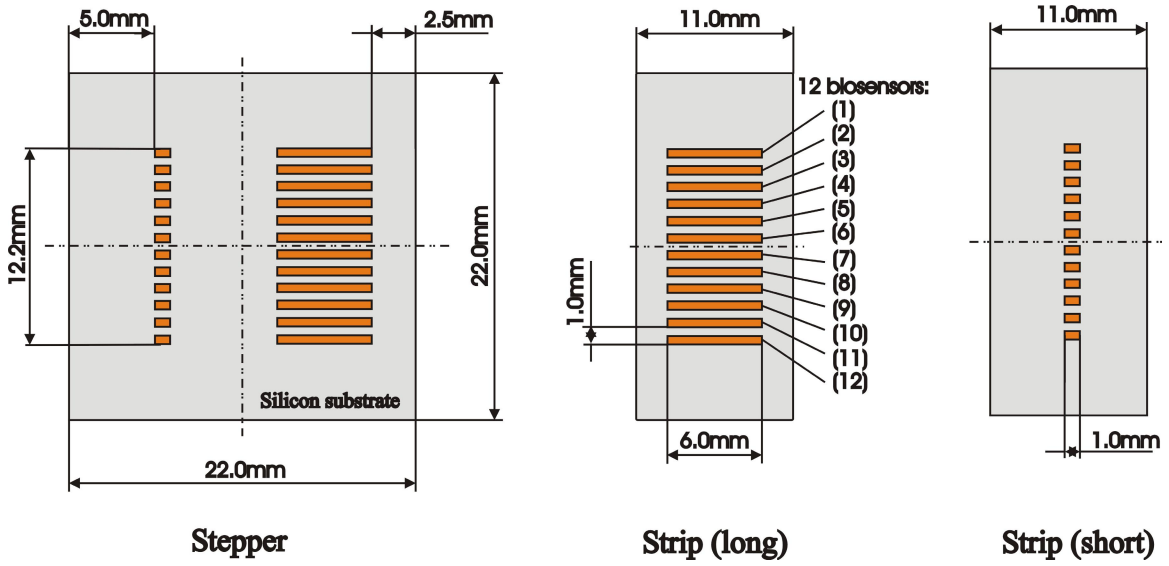

Figure 2. Layout of the sensor devices on Si wafer.

3. CHARACTERIZATION

The design of our WGM sensors is validated and characterized using the simulation model developed in Quan et al.[24], where we solved the two-dimensional time-harmonic EM wave equations using the finite element analysis. The slope of the tapered waveguide affects the total internal reflection inside the waveguide, especially in the area close to the microdisk. The simulation results of the EM fields for the straight and tapered waveguides are shown in Fig. 3 for both long and short waveguides. The electrical fields are shown in the left-hand side of the figures and the radiation energy density distributions are shown in the right-hand side of the figures. Because of the symmetric structure, only half of waveguide length is visualized. Microdisk was not incorporated in the simulations. It is seen that both the electrical field and radiation energy density are excellently confined inside the long straight waveguide. For the tapered waveguides, the leakage of electrical field in the short waveguide is apparent because of its relatively large slope. However, the radiation energy is still well confined.

The gap effects on the EM field and radiation power density field in the WGM sensors are demonstrated in Figs. 4 and 5, respectively, where three gap distances are selected for comparison, i.e., g = 200, 300, and 400nm. The diameter of the microdisks and the width of the waveguides keep constant at 15μm and 2μm, respectively. All three sensors are working under the same resonant mode (m = 118). It is observed that the EM field in the resonator becomes stronger and more radiation energy is stored in the resonator when the gap distance decreases. However, we should not conclude that a small gap is better for WGM resonance because we could not find any resonance phenomenon in the case of zero

gap distance. As a matter of fact, we found that, with the decrease of gap distance, the quality factor of the resonance decreases and the full width at half maximum (FWHM) of the resonant band increases as shown in Fig. 6. This means a poor quality of resonance. There may exist an optimal gap distance.

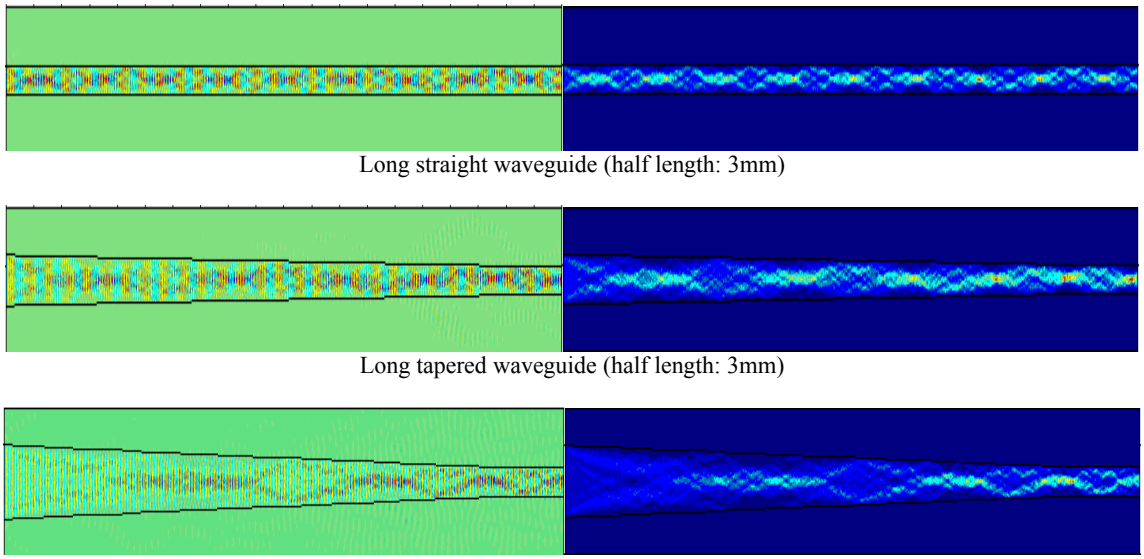

Long straight waveguide (half length: 3mm)

Long tapered waveguide (half length: 3mm)

Short tapered waveguide (half length: 0.5mm)

(a) Electrical field (b) Radiation energy density field

Figure 3. Comparisons of the simulated EM fields between different waveguides.

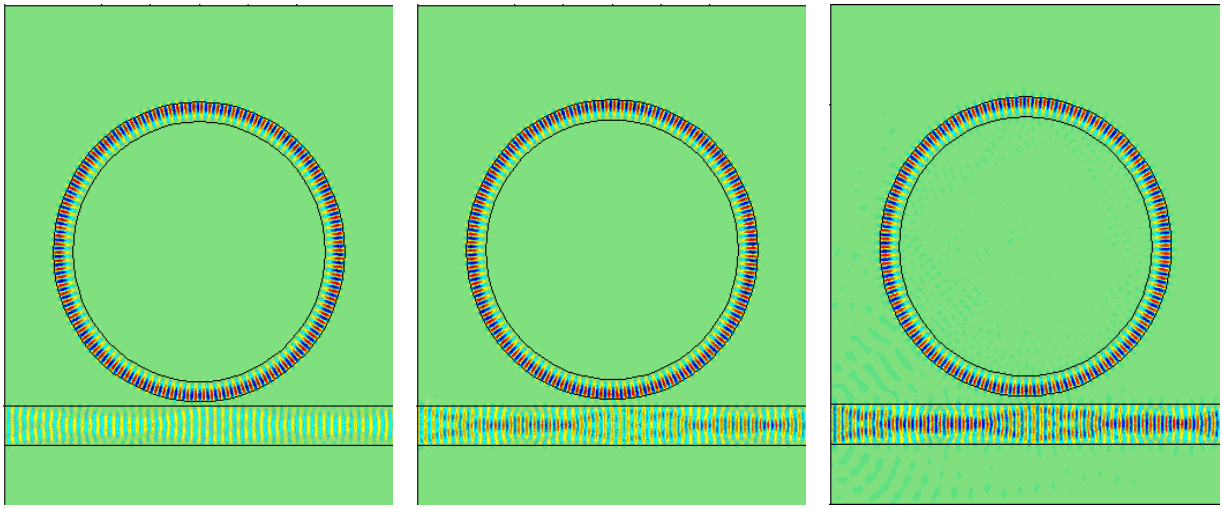

(a) g = 200nm (b) g = 300nm (c) g = 400nm

Figure 4. The electrical fields of WGM sensors on resonance with different gap distances.

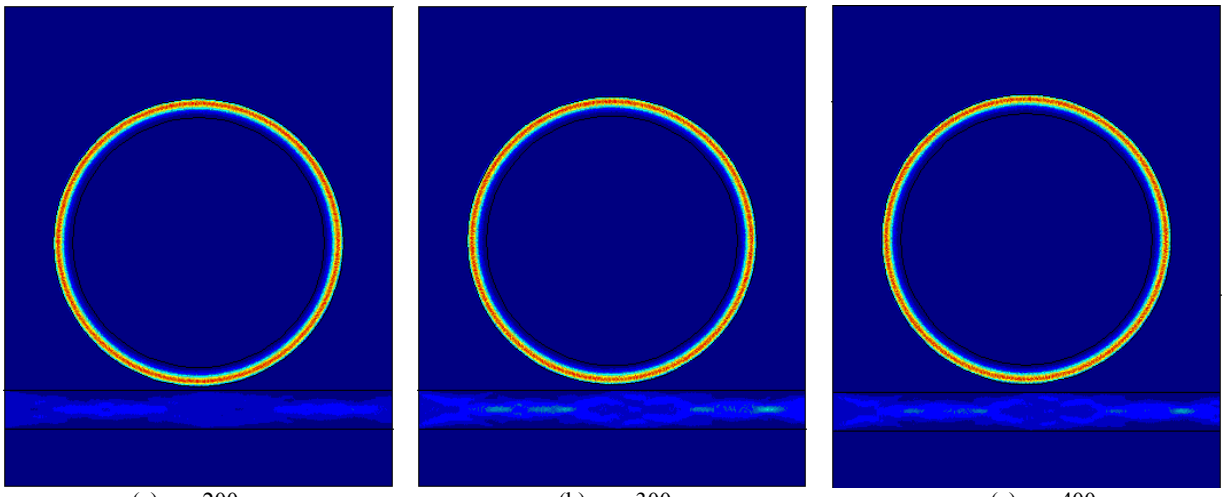

(a) g = 200nm (b) g = 300nm (c) g = 400nm

Figure 5. The radiation energy density distributions of WGM sensors on resonance with different gap distances.

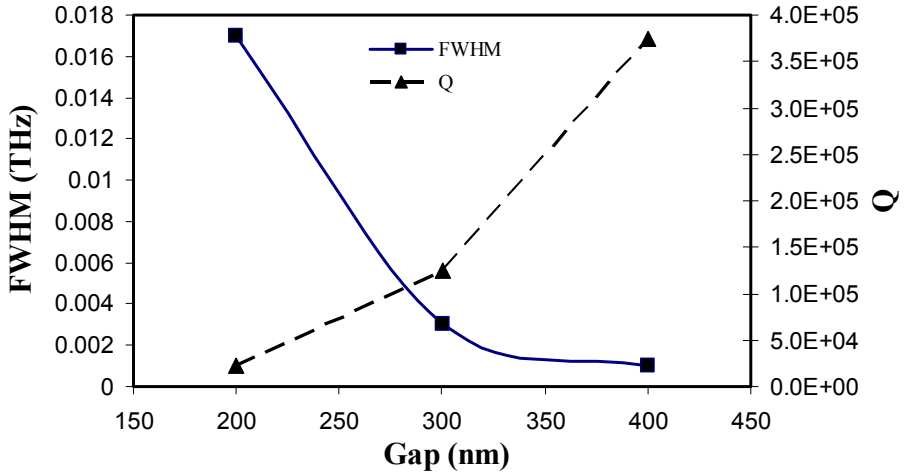

Figure 6. Gap effects on quality factor and FWHM.

4. FABRICATION

The minimum feature of the device is the gap between the waveguide and cavity. We fabricate the sensors using 248nm optical lithography and conventional silicon IC processing. The basic procedure is summarized below.

1) Deposition of buffer layer of SiO_2 on the silicon substrate.
2) Deposition of the Si_3N_4 layer.
3) Coat 1μm Shipley UV6 photoresist and expose wafer.
4) Etch the Si_3N_4 layer to make the structure of the miniature sensors and stop on oxide.
5) Strip photoresist and dice wafer.

Figure 7 shows a series of SEM photos of a finished sensor sample, focusing on the characteristics of the gap formed between the microdisk and waveguide. Figure 7(a) is the top view of the sensor after printing 230 nm gap on 1.3 μm resist in the first iteration of nanofabrication; and (b) details of the gap measured using SEM. We can have an overview

of the sample after etch through Figure 7(c), and further zoom in of the gap in (d). Figure 7(e) provides a close view of the etched sidewalls of the gap, from which surface roughness can be qualitatively evaluated.

Quantitative dimension characterization of the gap is also performed. Table 1 gives the data of top and down SEM measurements of the 12 sensors on one chip. Smallest gap width is found to be about 250nm.

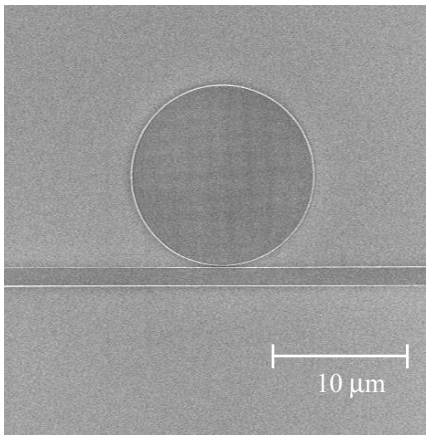

(a)

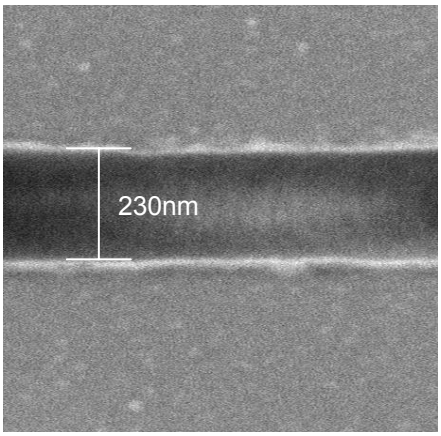

(b)

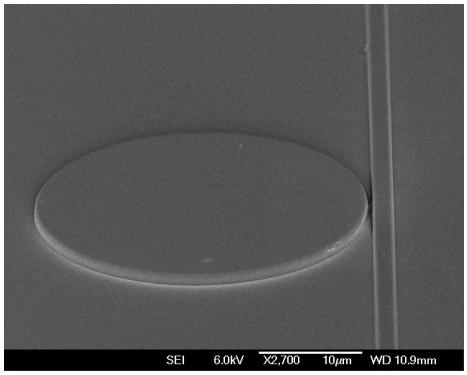

(c)

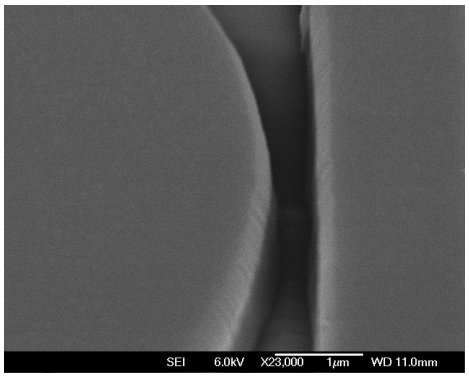

(d)

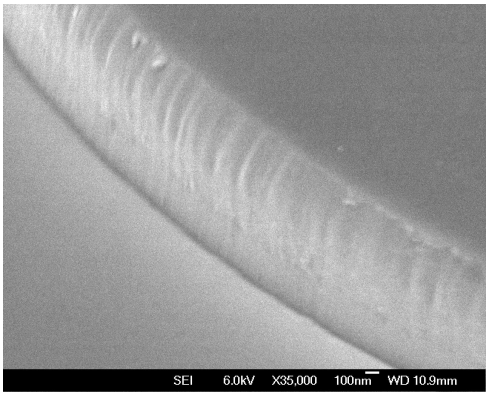

(e)

Figure 7. SEM images of a fabricated WGM sensor.

Table 1. Gap data from top and down SEM measurements

	Target CD (nm)	Actual CD bottom (nm)	Actual CD top (nm)
1	200	256.2	
2	300	345.8	481.2
3	400	470.9	578.1
4	200	254.2	
5	200	254.2	
6	200	259.4	
7	200	259.4	
8	300	333.3	
9	200	264.5	
10	300	354.2	
11	200	260.0	412.5
12	200	259.4	

5. CONCLUSIONS

We designed WGM miniature sensors based on the microdisk and waveguide coupling configuration. A number of sensors with different dimensions were fabricated in 1.3μm-thick Si_3N_4 film using 248nm optical lithography and conventional silicon IC processing. The designed gap separating the microdisk and waveguide varies between 200 and 400nm. The actual gaps vary between 250 to 580nm, and the fabricated gap separating the microdisk and waveguide is tapered from the bottom to the top of the device. The diameter of the microdisks in the design and actually fabricated sensors varies between 10 and 30μm. The width of the waveguide is either 2 or 3μm. Tapered waveguide is also designed and fabricated. In the fabrication, 8-inch wafers were used. The stepper die has an area of 22×22 mm^2. After the final processing step, the wafer was cut into chips of 11 x 22 mm^2. There are 12 parallel sensors in each chip and the sensors are equally separated with 1mm vertical distance. The length of the waveguides is 1mm in one chip, and 6mm in another chip. A simulation model was employed to characterize the EM and radiation energy density fields of the designed WGM sensors. It is found that WGM resonance quality is sensitive to the gap distance. The smaller the gap is, the stronger are the EM field and radiation energy density in the resonating microcavity. With the reduction of gap distance, the quality factor decreases and the FWHM of the resonant band increases.

ACKNOWLEDGMENTS

Z. Guo acknowledges the partial support of a 2003 - 2004 Academic Excellence Funds Award from Rutgers University and a NSF grant (CTS-0318001) to the project. The sponsor of device fabrication from the New Jersey Nanotechnology Consortium is gratefully appreciated.

REFERENCES

1. S. Arnold, "Microspheres, photonic atoms and the physics of nothing", *American Scientists*, **89**, 414-421 (2001).
2. A. Ashkin, and J.M. Dziedzic, "Observation of resonances in the radiation pressure on dielectric spheres," *Phys. Rev. Lett.*, **38**, 1351-1354 (1977).
3. C.F. Bohren, and D.R. Huffman, *Absorption and Scattering of Light by Small Particles*, John Wiley and Sons, New York, 1983.
4. H. Quan and Z. Guo, "Simulation of whispering-gallery-mode resonance shifts for optical miniature biosensors", *J. Quantitative Spectroscopy & Radiative Transfer*, in press (2005).
5. M. Cai, Q. Painter, K.J. Vahala, and P.C. Sercel, "Fiber-couppled microsphere laser", *Opt. Lett.*, **25**, 1430-1432 (2000).

6. M. Cai, and K.J. Vahala, "Highly efficient hybrid fiber coupled microsphere laser", *Opt. Lett.*, **26**, 884-886 (2001).

7. R.W. Boyd, and J.E. Heebner, "Sensitive disk resonator photonic biosensor", *Appl. Opt.*, **40**, 5742-5747 (2001).

8. B.E. Little, S.T. Chu, H.A. Haus, J. Foresi, and J.P. Laine, "Microring resonator channel dropping filters", *J. Lightwave Tech.*, **15**, 998-1005 (1997).

9. F.C. Blom, D.R. van Dijk, H.J Hoekstra, A. Driessen, and T.J.A. Popma, "Experimental study of integrated-optics micro-cavity resonators: toward an all-optical switching device," *Appl. Phys. Lett.*, **71**, 747-749 (1997).

10. S. Schiller, and R.L. Byer, "High-resolution spectroscope of whispering gallery modes in large dielectric spheres," *Opt. Lett.*, **16**, 1138-1140 (1991).

11. S. Blair and Y. Chen, "Resonant-enhanced evanescent-wave fluorescence biosensing with cylindrical optical cavities", *Appl. Opt.*, **40**, 570-582 (2001).

12. F. Vollmer, D. Braun, A. Libchaber, M. Khoshsima, I. Teraoka, and S. Arnold, "Protein detection by optical shift of a resonant microcavity", *Appl. Phys. Lett.*, **80**, 4057-4059 (2002).

13. I. Teraoka, S. Arnold, and F. Vollmer, "Perturbation approach to resonance shifts of whispering-gallery modes in a dielectric microsphere as probe of a surrounding medium", *J. Opt. Soc. Am. B*, **20**, 1937-1946 (2003).

14. S. Arnold, M. Khoshsima, I. Teraoka, and F. Vollmer, "Shift of whispering-gallery modes in microspheres by protein adsorption", *Opt. Lett.*, **28**, 272-274 (2003).

15. A. Serpenguzel, S. Arnold, and G. Griffel, "Excitation of resonances of microspheres on an optical fiber," *Opt. Lett.*, **20**, 654-656 (1995).

16. J.C. Knight, G. Cheung, F. Jacques, and T.A. Birks, "Phase-matched excitation of whispering-gallery-mode resonances by a fiber taper", *Opt. Lett.*, **22**, 1129-1131 (1997).

17. J.P. Laine, B.E. Little, H.A. Haus, "Etch-eroded fiber coupler for whispering-gallery-mode excitation in high-Q silica microspheres", *IEEE Photonics Tech. Lett.*, **11**, 1429-1430 (1999).

18. F. Lissillour, D. Messager, G. Stephan, and P. Feron, "Whispering-gallery-mode laser at 1.56 μm excited by a fiber taper", *Opt. Lett.*, **26**, 1051-1053 (2001).

19. J.P. Zhang, D.Y. Chu, S.L. Wu, S.T. Ho, W.G. Bi, C.W. Tu, and R.C. Tiberio, "Photonic-wire laser", *Phys. Rev. Lett.*, **75**, 2678-2681 (1995).

20. J.P Laine, C. Tapalian, B. Little, and H. Haus, "Acceleration sensor based on high-Q optical microsphere resonator and pedestal antiresonant reflecting waveguide coupler", *Sensors & Actuators A: Physical*, **93**, 1-7 (2001).

21. D.J.W. Klunder, E. Krioukov, F.S. Tan, T. Van Der Veen, H.F. Bulthuis, G. Sengo, C. Otto, H.J.W.M. Hoekstra, and A. Driessen, "Vertically and laterally waveguide-coupled cylindrical microresonators in Si_3N_4 on SiO_2 technology", *Appl. Phys. B*, **73**, 603-608 (2001).

22. E. Krioukov, D.J.W. Klunder, A. Driessen, J. Greve, and C. Otto, "Integrated optical microcavities for enhanced evanescent-wave spectroscopy", *Opt. lett.*, **27**, 1504-1506 (2002).

23. A. Belarouci, K.B. Hill, Y. Liu, Y. Xiong, T. Chang, and A.E. Craig, "Design and modeling of waveguide-coupled microring resonator", *J. Luminescence*, **94-95**, 35-38 (2001).

24. H. Quan, Z. Guo, and S. Pau, "Parametric studies of whispering-gallery mode resonators", *Proceedings of SPIE*, vol. 5593, (in press), 2004.

25. T.R Hsu, *MEMS & Microsystems Design and Manufacture*, McGraw-Hill, 2002

26. E. D. Palik, *Handbook of Optical Constants of Solids*, Academic Press, Orlando, 1985

27. P. Rabiei, W.H. Steier, C. Zhang and L.R. Dalton, "Polymer micro-ring filters and modulators", *J. Lightwave Tech.*, **20**, 1968-1975 (2002).